

# Bifunctional Inhibitors as a New Tool To Reduce Cancer Cell Invasion by Impairing MMP-9 Homodimerization

Elisa Nuti,<sup>†</sup> Lea Rosalia,<sup>†</sup> Doretta Cuffaro,<sup>†</sup> Caterina Camodeca,<sup>†</sup> Chiara Giacomelli,<sup>†</sup> Eleonora Da Pozzo,<sup>†</sup> Tiziano Tuccinardi,<sup>†</sup> Barbara Costa,<sup>†</sup> Claudia Antoni,<sup>†,‡</sup> Laura Vera,<sup>‡</sup> Lidia Ciccone,<sup>†</sup> Elisabetta Orlandini,<sup>†</sup> Susanna Nencetti,<sup>†</sup> Vincent Dive,<sup>‡</sup> Claudia Martini,<sup>†</sup> Enrico A. Stura,<sup>‡</sup> and Armando Rossello<sup>\*,†</sup>

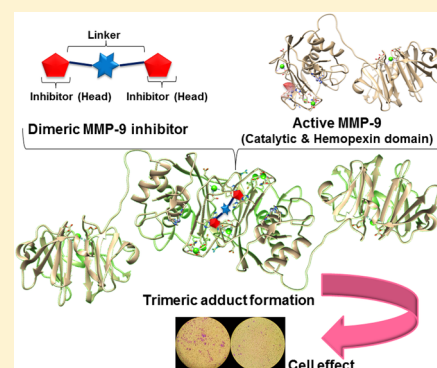
<sup>†</sup>Dipartimento di Farmacia, Università di Pisa, Via Bonanno 6, 56126 Pisa, Italy

<sup>‡</sup>CEA, iBiTec-S, Service d'Ingénierie Moléculaire des Protéines, CE-Saclay, 91191 Gif sur Yvette Cedex, France

## Supporting Information

**ABSTRACT:** Protein homodimers play important roles in physiological and pathological processes, including cancer invasion and metastasis. Recently, MMP-9 natural homodimerization via the PEX domain has been correlated with high migration rates of aggressive cancer cells. Here we propose that bifunctional MMP-9 inhibitors designed to impair natural MMP-9 homodimerization promoted by PEX–PEX interactions might be an effective tool to fight cancer cell invasion. Elaborating a previously described dimeric hydroxamate inhibitor **1**, new ligands were synthesized with different linker lengths and branch points. Evaluation of the modified bifunctional ligands by X-ray crystallography and biological assays showed that **7** and **8** could reduce invasion in three glioma cell lines expressing MMP-9 at different levels. To rationalize these results, we present a theoretical model of full-length MMP-9 in complex with **7**. This pioneering study suggests that a new approach using MMP-9 selective bifunctional inhibitors might lead to an effective therapy to reduce cancer cell invasion.

**KEYWORDS:** Bifunctional inhibitors, MMP-9 homodimerization, glioblastoma multiforme, X-ray crystallography



Matrix metalloproteinases (MMPs) are a family of zinc-dependent endopeptidases responsible for the hydrolytic cleavage of all components of extracellular matrix (ECM), such as collagens, laminin, fibronectin, elastin, and proteoglycans.<sup>1</sup> In the last decades, MMPs have been considered potential therapeutic targets for various diseases such as cancer and inflammation. Unfortunately, the considerable efforts spent developing synthetic MMP inhibitors have not been rewarded in clinical trials.<sup>2</sup> The high degree of homology among MMP family members and insufficient appreciation for complexity of MMP functions can explain these failures.<sup>3</sup> The challenge is to devise new strategies to obtain selective compounds that should have less side effects.<sup>4</sup> Among all MMPs, here we focus on gelatinase B (MMP-9), that is involved in a variety of pathological processes from cancer invasion, metastasis, and angiogenesis, to cardiovascular and neurological diseases.<sup>5</sup> Not all these effects are related to its proteolytic activity. Enhanced cell migration is promoted by dimerization mediated by the hemopexin (PEX) domain.<sup>6</sup> MMP-9 is currently the only secreted MMP known to form either homodimers or heterodimers. PEX driven homodimerization of MMP-9 has been correlated with high migration rates of aggressive cancer cells. Heterodimerization with CD44, or homing cell adhesion molecule (HCAM), was shown to play a key role in MMP-9 enhanced cell migration. While the MMP-9 homodimeric

interaction involves blade IV of the PEX domain, the heterodimeric MMP9-CD44 interactions are mediated by blade I. Peptides designed to interfere with MMP-9 homodimerization abrogated MMP-9 enhanced cell migration in COS-1 cells<sup>7</sup> and a small molecule able to bind selectively to PEX was able to reduce MDA-MB-435 tumor growth and inhibit lung metastasis in vivo.<sup>8</sup> Our approach to reduce cancer cell migration and invasion envisions interfering with MMP-9 natural homodimerization. Through the binding of bifunctional ligands to the catalytic site of two MMP-9 monomers we attempt to impair MMP-9 natural homodimerization mediated by PEX–PEX interactions by preventing the PEX domains to approach each other.

Dimeric inhibitors have already been studied in several fields of medicinal chemistry, such as kinase inhibitors, HIV protease inhibitors, cholinesterase inhibitors and MMP inhibitors,<sup>9</sup> with promising results. Starting from a potent MMP-2, -9, and -14 twin hydroxamate inhibitor **1**<sup>10</sup> (Figure 1), endowed with a reduced cell cytotoxicity, we aimed to develop new bifunctional ligands more selective for MMP-9 over other MMP family members. The successful crystallization and structure determi-

Received: November 7, 2016

Accepted: February 7, 2017

Published: February 7, 2017

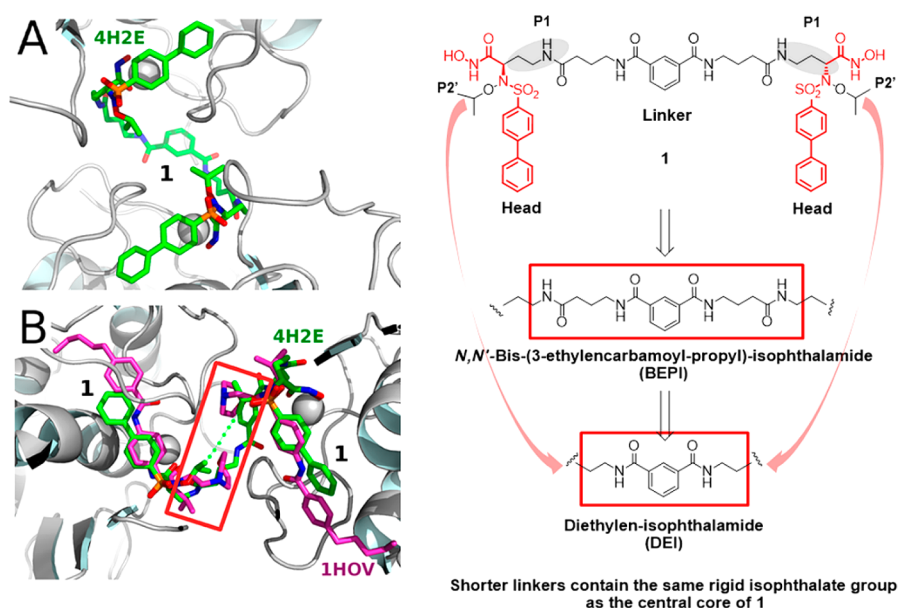
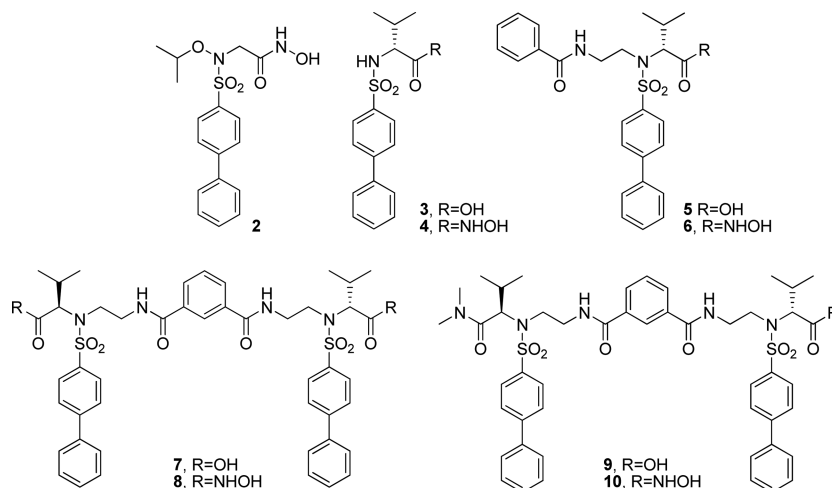


**Figure 1.** New bifunctional inhibitors design from the crystallographic structure of the complex 1-MMP-9 catalytic domain. (A) Crystal structure of MMP-9 (PDB 4H2E)<sup>11</sup> in complex with 1 (green) showing how the long linker spans the distance between the two MMP-9 catalytic domains present in the crystal lattice. (B) Superimposition of the SC-74020 (magenta) complex with-MMP-2 from the NMR structure (PDB 1HOV)<sup>13</sup> on each of the two crystallographic cat-MMP-9. The shortest distance between the two SC-74020 is only 3.6 Å (red box). Given the similarity of the central cores around the ZBG of 1 and SC-74020, changing the linkage point from P1 to P2' should yield a shorter DEI linker that might induce the same MMP-9 dimer observed in the crystal.

#### Chart 1. Chemical Structures of New Compounds 5–10 and the Known Compounds 2–4



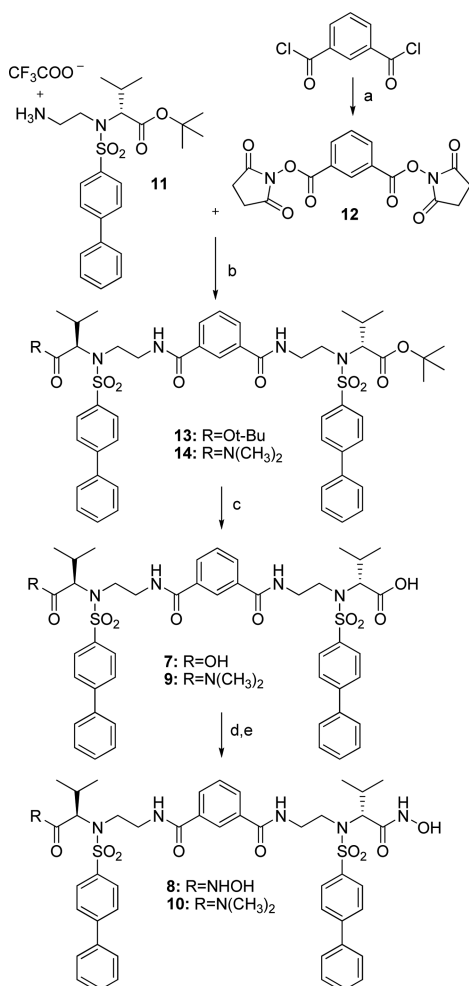
nation of the complex of 1 (green in Figure 1A) with MMP-9 catalytic domain (cat-MMP9) at 2.9 Å resolution (PDB 4H2E)<sup>11</sup> have provided a structural basis to understand the dimerization mode. In this complex, 1 unites two MMP-9 catalytic domains forming a trimeric adduct. The symmetrical linker, *N,N'*-bis(3-ethylencarbamoyl-propyl)-isophthalamide (BEPI), ties together two moieties of the known monomeric inhibitor 2<sup>12</sup> (Chart 1) in the P1 position. The structure shows that the shortest distance between the two inhibitor heads of 1 in P2' position (the terminal carbon atoms of the oxypropyl group) is 6.5 Å, suggesting that a shorter linker and an alternative branch point may improve the stability of the complex. Superimposition of compound SC-74020,<sup>13</sup> chosen for the similarity of its central core around the ZBG with respect to 1, in complex with MMP-2 on the complex of 1 with MMP-9 helped design the new branch point and define the

linker length (see Figure 1B). On this basis, compounds 7–10, (Chart 1) were synthesized with a shorter diethylene-isophthalamide (DEI) linker in P2' position. The new inhibitors were tested in enzymatic assays and the structure of their complex with MMP-9 determined by X-ray crystallography to compare the effects of the carboxylate and hydroxamate-based zinc-binding groups (ZBGs). The carboxylate inhibitor 3<sup>14</sup> and its hydroxamate analogue 4<sup>15</sup> (Chart 1) represent the two inhibitor heads that are linked in the bifunctional inhibitor. For completion, we also synthesized monomeric compounds 5 and 6 (Chart 1) with a P2' *N*-ethylene-benzamide side chain. Without this chain that represents a superimposable structural portion of the DEI linker (Figure S1), in 5 and 6 the effects of the inhibitor dimerization on potency and selectivity for MMP-9 cannot be compared objectively. The monovalent derivatives 9 and 10

containing a dimethylamide group unable to chelate the catalytic zinc ion were also synthesized as additional controls.

Compounds 7–10 were synthesized as reported in Scheme 1. Salt 11 has been prepared as previously described.<sup>16</sup> Di-NHS

### Scheme 1. Synthesis of P2' Dimers 7–10<sup>a</sup>



<sup>a</sup>Reagents and conditions: (a) *N*-hydroxysuccinimide, Et<sub>3</sub>N, THF, rt, 2 h; (b) DIPEA, DMF, rt, 16 h; (c) TFA, CH<sub>2</sub>Cl<sub>2</sub>, 0 °C, 5 h; (d) TBDMSiONH<sub>2</sub>, EDC, CH<sub>2</sub>Cl<sub>2</sub>, rt, 16 h; (e) TFA, CH<sub>2</sub>Cl<sub>2</sub>, 0 °C, 5 h.

(*N*-hydroxysuccinimido) activated ester 12 was obtained by reaction of isophthaloyl dichloride with *N*-hydroxysuccinimide using triethylamine as base. Activated ester 12 was added to a DMF solution of 11 in the presence of *N,N*-diisopropylethylamine (DIPEA) to give the di-*tert* butyl ester (*R,R*)-13 and the *N,N*-dimethylamido derivative 14, which were separated by flash chromatography. The corresponding carboxylic acid derivatives 7 and 9 were obtained by *tert*-butyl group cleavage with trifluoroacetic acid (TFA). These carboxylates were converted into the corresponding hydroxamates 8 and 10 by condensation with *O*-(*tert*-butyldimethylsilyl)hydroxylamine (TBDMSiONH<sub>2</sub>) to give the silyl intermediates and subsequent deprotection of the hydroxamate moiety with TFA.

Monomer derivatives 5 and 6 were synthesized as reported in the Supporting Information (Scheme S1).

All the inhibitors described in the present study, 5–10, were tested *in vitro* on the target enzyme MMP-9 and on some other MMPs (MMP-1, MMP-2, and MMP-14) by fluorometric assay.

MMP-2 and MMP-14 were chosen because they are widely expressed in many kinds of tumors together with MMP-9,<sup>17</sup> while inhibition of MMP-1 is believed to be responsible for the musculoskeletal syndrome clinically observed with the use of broad-spectrum MMP inhibitors.<sup>18</sup> The previously described twin hydroxamate 1 was used as reference compound. Results are reported in Table 1 as IC<sub>50</sub> values (nM). The shorter linker

**Table 1.** *In Vitro*<sup>a</sup> Inhibitory Activity (IC<sub>50</sub>, nM) of New Compounds 5–10 and the Reference Compound 1 on MMPs

| compd | MMP-1 | MMP-2 | MMP-9 | MMP-14 |
|-------|-------|-------|-------|--------|
| 1     | 5200  | 20    | 38    | 116    |
| 5     | 16000 | 170   | 510   | 1830   |
| 6     | 13    | 0.16  | 2.5   | 23     |
| 7     | 11800 | 63    | 26    | 2200   |
| 8     | 280   | 10    | 5.5   | 250    |
| 9     | 2050  | 110   | 34    | 850    |
| 10    | 1600  | 107   | 41    | 900    |

<sup>a</sup>Enzymatic data are mean values for three independent experiments performed in duplicate. SD were generally within ±10%.

and the repositioning of the branch point from P1 to P2' led to a 7-fold increase in potency toward MMP-9, evident from the comparison of the new dimeric hydroxamate 8 to 1. Although this improvement in potency was broad-spectrum and thus accompanied by a loss of selectivity, the dicarboxylate analogue of 8, compound 7, was found to have nanomolar activity toward MMP-9 (IC<sub>50</sub> = 26 nM) and a selectivity over other MMPs better than 1. In particular, 7 had a 450-fold selectivity for MMP-9 over MMP-1.

Comparing 7 with its carboxylate monomer 5, the latter showed a drop of inhibitory activity for MMP-9 (IC<sub>50</sub> = 510 nM) and also a decreased selectivity. Its corresponding hydroxamate monomer, 6, exhibited a nanomolar activity on all tested enzymes, thus losing any selectivity for MMP-9. Finally, also monovalent derivatives 9 and 10 showed a worse selectivity profile than 7 despite their similar affinity for MMP-9, indicating that the nature of the ZBG and the presence of a bivalent functionality are both important for improving MMP-9 selectivity (Table 1).

Once the X-ray crystallographic structure of the complex between 8 and MMP-9 was solved (PDB 4H82)<sup>11</sup> its superimposition on the complex between 1 and MMP-9 showed that the bivalent ligands overlapped well as far as their inhibitor moieties were concerned and that the shorter linker would hinder dissociation. This alternative linkage gives the same trimeric adduct obtained for 1 but with a stricter geometry, conducive to greater potency as expected from its design (Figure 2A). From this superimposition it is evident that the P2' linkage using a DEI linker gives a correct distance and geometry of the twin inhibitor (compound 8, light blue) able to form a stable trimeric adduct with MMP-9. The crystal structures provide a possible explanation for the binding data, in terms of linker flexibility, different dimerization modes for each MMP and subtle variations in ligand positioning when analogue ligands with different ZBGs (7 and 8, Figure 2) are compared. Regarding the two monovalent derivatives of 7 and 8, the monoacid 9, and the monohydroxamate 10, these were totally unable to give trimers in the crystals with MMP-9. This fact is easily rationalized considering that, despite having a dimeric structure, they possess a dimethylamide group unable

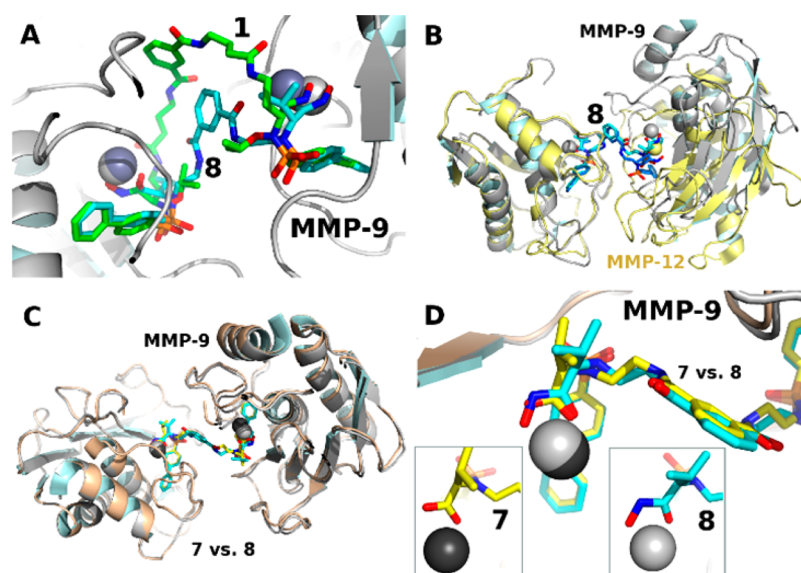


**Figure 2.** Superimposition of bifunctional ligands 1, 7, and 8. (A) The shortening and repositioning of the branch point results in reduced geometrical freedom (1, PDB 4H2E, green; 8 PDB 4H82, cyan).<sup>11</sup> (B) Comparison of the dimerization mode of MMP-9 (gray ribbons) and MMP-12 (PDB 4H49, yellow)<sup>11</sup> to highlight that it is unlikely that different MMPs will share dimerization modes. (C) Superposition on C $\alpha$  atoms of residues from the cat-MMP-9: molecule B of PDB 4HMA,<sup>11</sup> orange cartoon with ligand 7 (yellow sticks) was superposed with molecule B of PDB 4H82,<sup>11</sup> gray cartoon with ligand 8 in cyan sticks. Changing the ZBG from the hydroxamate of 8 to carboxylate of 7 in the MMP-9 complex alters only slightly the overall linker-induced trimer. (D) Zoom on the MMP-9 zinc atom to highlight the subtle changes induced by changing the ZBG. The position of the zinc in the hydroxamate complex, 8 (gray) differs slightly from that in the MMP-9 carboxylate complex 7 (black). The difference in the zinc position and in the chelation mode of the hydroxamate moiety compared to the carboxylate alters only slightly the positioning of the linker, which at long distance changes the dimerization. Such subtle differences impact strongly on affinity and selectivity.

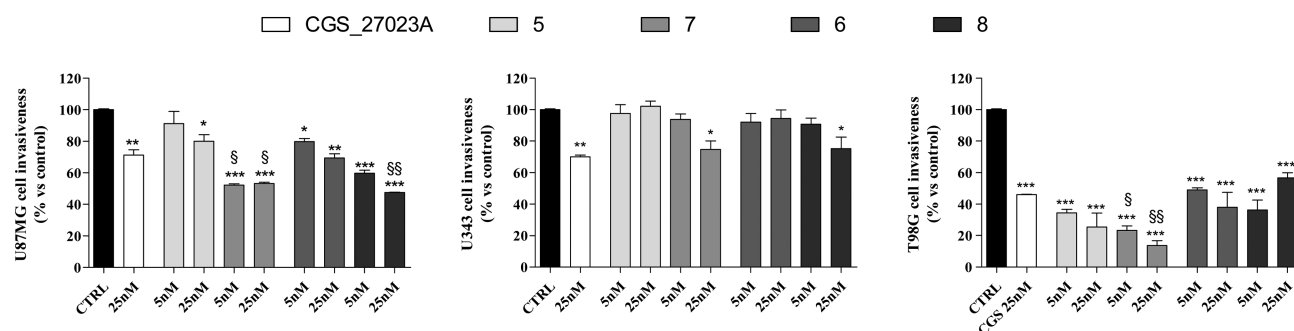


**Figure 3.** MMP inhibitors effects on cell invasiveness. The invasiveness of treated and untreated (DMSO, control) cells (U87MG, U343MG, and T98G) were assessed in matrigel basement membrane matrix. Cells able to invade were visualized by crystal violet probe and counted by the means of ImageJ software. Data are presented as the mean  $\pm$  SEM, and derived from at least three independent experiments done in duplicate. \* $p < 0.05$ ; \*\* $p < 0.01$ ; \*\*\* $p < 0.005$ ; \*Significance vs control using ANOVA with post hoc Newman–Keuls test. § $p < 0.05$ ; §§ $p < 0.01$ ; §§significance vs CGS27023A, using ANOVA with post hoc Newman–Keuls test.

to chelate the catalytic zinc ion of the MMP-9 catalytic domain. Of course, purified recombinant enzymes may not be ideal to assess properties of bifunctional inhibitors. Therefore, in order to prove a possible role of these twin MMP inhibitors in interfering with protein–protein interactions, compound 7 and its analogues 5, 6, and 8 were evaluated in a cancer cell invasion assay where MMP-9 homodimerization and heterodimerization are possible. In particular, following our previous studies on gliomas,<sup>19,20</sup> we chose three human glioblastoma multiforme (hGBM) cell lines: U87MG, T98G, and U343MG, known in literature for expressing different levels of MMP-9.<sup>21</sup> First, the expression of MMP-9 was analyzed by RT-PCR (Figure S2). As expected, the different cell lines showed different mRNA expression levels of MMP-9, which was highly expressed in U87MG and poorly expressed in U343MG.

Then, the MMP inhibitors effects on cell proliferation were evaluated by MTS assay, and none of the tested compounds showed significant toxic effects on cells after 24 h of treatment at nanomolar concentrations, as shown in Figure S3. Finally, compounds 5–8 were tested in a cancer cell invasion assay at 5 and 25 nM. Treatment for 24 h with the new MMP inhibitors resulted in a marked reduction in glioma cell invasion through the matrigel basement membrane matrix in U87MG and T98G cell (Figure 3). Dimeric inhibitors 7 and 8 were the most effective in reducing invasiveness (statistical significance  $p < 0.0001$ ), considerably more than their corresponding monomeric inhibitors, 5 and 6, that have an ability to reduce invasiveness similar to the broad-spectrum MMP inhibitor CGS27023A ( $p < 0.01$ ), used as control. Otherwise in U343MG cells, only the treatment with the highest dose of 7 and 8 showed a reduction in cell invasion through the matrigel,

with a lesser extent than the standard compound CGS27023A (Figure 3). This fact seems to suggest a strong involvement of MMP-9 in this anti-invasive effect because, as seen above, U343MG cells have a low expression level of MMP-9 and therefore are less sensitive to the effect of these inhibitors.

All the data on living cells taken together supports the starting hypothesis that the selective bifunctional inhibitors interfere with natural protein–protein interactions. Independently of the inhibitory activity measured on isolated enzymes, the dimeric compounds 7 and 8 give the best results in the cell invasion assays suggesting the existence of a mechanism that is different from what would be expected from the simple inhibition of MMP-9 catalytic activity. For this reason and for its good MMP-9 selectivity and ability to reduce invasion of all glioma cell lines, the dicarboxylate dimer 7 was chosen for further studies. A preliminary analysis of the *in vitro* ADME properties of 7 has been performed as reported in the Supporting Information. The X-ray crystallographic structure of 7 complexed with two MMP-9 catalytic domains (PDB 4HMA)<sup>11</sup> strongly supports the hypothesis that this twin inhibitor is likely to interact with two MMP-9 monomers and force the same dimeric arrangement observed in the crystal structure. To understand whether the disposition of the two catalytic domains could be in an agreement with a possible not natural homodimerization of full-length MMP-9, computational studies were carried out. The X-ray crystallographic structure of the complex of 7 with the MMP-9 catalytic domain was used as a starting point for the calculations. The full-length MMP-9-MMP-9 trimer was reconstructed and subjected to 100 ns of molecular dynamic simulation. As shown in Figure 4, the catalytic domain disposition reported in the crystallographic

structure was fully compatible with the hypothesized trimeric adduct. The analysis of this structure suggested that the two fibronectin domains might be in tight contact forming favorable H-bonds and van der Waals interactions. In particular, a tryptophan network at the surface contact of the third fibronectin domain of the two chains was noted as especially favorable (Figure S4). A  $\Pi$ – $\Pi$  stacking interaction is formed between W373.A and W373.B, with these two residues also engaging in a T-shaped interaction with W386.B and W386.A, respectively. With regards to the PEX domains, it is predicted that ligand induced dimerization would position them at the opposite sides of the trimer, different from what is known for the natural MMP-9 homodimer.<sup>22,23</sup>

With the ligand bound to two MMP-9 monomers, they would be unable to interact with each other. Therefore, this computational model supports the hypothesis that bifunctional MMP-9 inhibitors might impair MMP-9 natural homodimerization by distancing the PEX domains from each other.

In conclusion we have described a new approach with results that show reduced cancer cell invasion rates when bifunctional MMP-9 inhibitors are used. Computational studies based on the crystallographic structures of MMP-9 in complex with the twin inhibitors suggest a mode of action where ligand-induced dimerization is incompatible with natural protein–protein interactions that drive MMP-9 homodimerization. In order to confirm this hypothesis further experimental proofs are required. For instance, site-mutation mutagenesis experiments on key residues, suggested as responsible for protein–protein interactions, might provide important insights. The results from such investigations would allow us to better exploit its potentiality so as to be able to formulate an alternative and safer approach to reduce cancer migration and invasion in those cancers where MMP-9 is overexpressed.

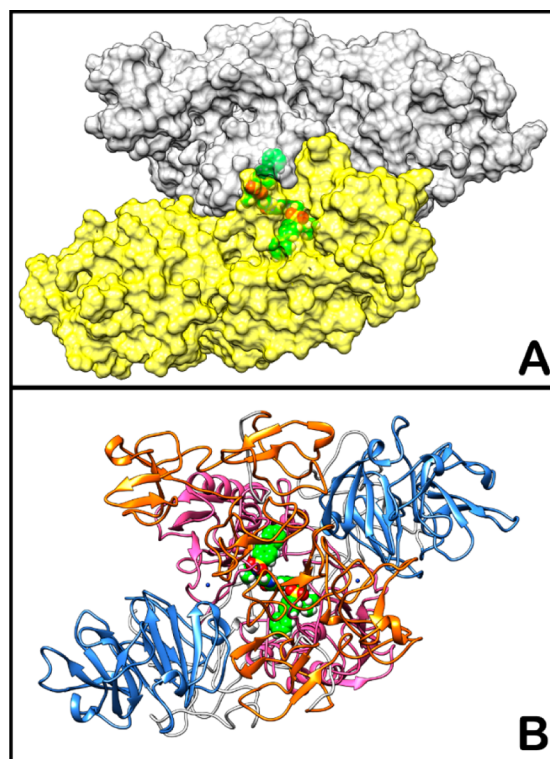


**Figure 4.** Proposed trimeric adduct MMP-9-7-MMP-9. Surface visualization (A) and ribbon representation (B) (domains colors: pink, catalytic; orange, fibronectin; blue, hemopexin). Compound 7 is colored green.

## ■ ASSOCIATED CONTENT

### 📄 Supporting Information

The Supporting Information is available free of charge on the ACS Publications website at DOI: 10.1021/acsmchemlett.6b00446.

Supplementary figures, experimental details, compound characterization, and abbreviations (PDF)

## ■ AUTHOR INFORMATION

### Corresponding Author

\*E-mail: armando.rossello@farm.unipi.it.

### ORCID

Elisa Nuti: 0000-0003-2669-5376

Tiziano Tuccinardi: 0000-0002-6205-4069

Claudia Martini: 0000-0001-9379-3027

Armando Rossello: 0000-0002-6795-8091

### Author Contributions

The manuscript was written through contributions of all authors. All authors have given approval to the final version of the manuscript.

### Funding

This work was supported by “Fondi di Ateneo-University of Pisa” years 2014 and 2015 (S.N., E.N., E.O., and A.R.) and by the Unipi project P.R.A. 2016\_27.

### Notes

The authors declare no competing financial interest.

## ■ ACKNOWLEDGMENTS

We are grateful to the ESRF and SOLEIL and to their staff for allocation of beam time and assistance during data collection. The authors gratefully acknowledge Prof. Gillian Murphy, University of Cambridge, for critical reading of the manuscript.

## ■ REFERENCES

- (1) Nagase, H.; Woessner, J. F. Matrix metalloproteinases. *J. Biol. Chem.* **1999**, *274*, 21491–21494.
- (2) Coussens, L. M.; Fingleton, B.; Matrisian, L. M. Matrix metalloproteinase inhibitors and cancer: Trials and tribulations. *Science* **2002**, *295*, 2387–2392.
- (3) Vandenbroucke, R. E.; Libert, C. Is there new hope for therapeutic matrix metalloproteinase inhibition? *Nat. Rev. Drug Discovery* **2014**, *13*, 904–927.
- (4) Santamaria, S.; Nuti, E.; Cercignani, G.; La Regina, G.; Silvestri, R.; Supuran, C. T.; Rossello, A. Kinetic characterization of 4,4'-biphenylsulfonamides as selective non-zinc binding MMP inhibitors. *J. Enzyme Inhib. Med. Chem.* **2015**, *30*, 947–954.
- (5) Vandooren, J.; Van den Steen, P. E.; Opdenakker, G. Biochemistry and molecular biology of gelatinase B or matrix metalloproteinase-9 (MMP-9): the next decade. *Crit. Rev. Biochem. Mol. Biol.* **2013**, *48*, 222–272.
- (6) Dufour, A.; Sampson, N. S.; Zucker, S.; Cao, J. Role of the hemopexin domain of matrix metalloproteinases in cell migration. *J. Cell. Physiol.* **2008**, *217*, 643–651.
- (7) Dufour, A.; Zucker, S.; Sampson, N. S.; Kucsu, C.; Cao, J. Role of matrix metalloproteinase-9 dimers in cell migration: design of inhibitory peptides. *J. Biol. Chem.* **2010**, *285*, 35944–35956.
- (8) Dufour, A.; Sampson, N. S.; Li, J.; Kucsu, C.; Rizzo, R. C.; Deleon, J. L.; Zhi, J.; Jaber, N.; Liu, E.; Zucker, S.; Cao, J. Small-molecule anticancer compounds selectively target the hemopexin domain of matrix metalloproteinase-9. *Cancer Res.* **2011**, *71*, 4977–4988.
- (9) Wang, J.; Radomski, M. W.; Medina, C.; Gilmer, J. F. MMP inhibition by barbiturate homodimers. *Bioorg. Med. Chem. Lett.* **2013**, *23*, 444–447.
- (10) Rossello, A.; Nuti, E.; Catalani, M. P.; Carelli, P.; Orlandini, E.; Rapposelli, S.; Tuccinardi, T.; Atkinson, S. J.; Murphy, G.; Balsamo, A. A new development of matrix metalloproteinase inhibitors: twin hydroxamic acids as potent inhibitors of MMPs. *Bioorg. Med. Chem. Lett.* **2005**, *15*, 2311–2314.
- (11) Antoni, C.; Vera, L.; Devel, L.; Catalani, M. P.; Czarny, B.; Cassar-Lajeunesse, E.; Nuti, E.; Rossello, A.; Dive, V.; Stura, E. A. Crystallization of bi-functional ligand protein complexes. *J. Struct. Biol.* **2013**, *182*, 246–254.
- (12) Rossello, A.; Nuti, E.; Orlandini, E.; Carelli, P.; Rapposelli, S.; Macchia, M.; Minutolo, F.; Carbonaro, L.; Albini, A.; Benelli, R.; Cercignani, G.; Murphy, G.; Balsamo, A. New N-arylsulfonyl-N-alkoxyaminoacetohydroxamic acids as selective inhibitors of gelatinase A (MMP-2). *Bioorg. Med. Chem.* **2004**, *12*, 2441–2450.
- (13) Feng, Y.; Likos, J. J.; Zhu, L.; Woodward, H.; Munie, G.; McDonald, J. J.; Stevens, A. M.; Howard, C. P.; De Crescenzo, G. A.; Welsch, D.; Shieh, H. S.; Stallings, W. C. Solution structure and backbone dynamics of the catalytic domain of matrix metalloproteinase-2 complexed with a hydroxamic acid inhibitor. *Biochim. Biophys. Acta, Proteins Proteomics* **2002**, *1598*, 10–23.
- (14) A. Rossello, A.; Nuti, E.; Tuccinardi, T.; Orlandini, E. Arylsulphonamidic dimers as metalloprotease inhibitors. PCT. WO2010010080, 2010.
- (15) Xiong, Y.; Wiltsie, J.; Woods, A.; Guo, J.; Pivnichny, J. V.; Tang, W.; Bansal, A.; Cummings, R. T.; Cunningham, B. R.; Friedlander, A. M.; Douglas, C. M.; Salowe, S. P.; Zaller, D. M.; Scolnick, E. M.; Schmatz, D. M.; Bartizal, K.; Hermes, J. D.; MacCoss, M.; Chapman, K. T. The discovery of a potent and selective lethal factor inhibitor for adjunct therapy of anthrax infection. *Bioorg. Med. Chem. Lett.* **2006**, *16*, 964–968.
- (16) Nuti, E.; Cuffaro, D.; D'Andrea, F.; Rosalia, L.; Tepshi, L.; Fabbri, M.; Carbotto, G.; Ferrini, S.; Santamaria, S.; Camodeca, C.; Ciccone, L.; Orlandini, E.; Nencetti, S.; Stura, E. A.; Dive, V.; Rossello, A. Sugar-based arylsulfonamide carboxylates as selective and water-soluble Matrix Metalloproteinase-12 inhibitors. *ChemMedChem* **2016**, *11*, 1626–1637.
- (17) Deryugina, E. I.; Quigley, J. P. Matrix metalloproteinases and tumor metastasis. *Cancer Metastasis Rev.* **2006**, *25*, 9–34.
- (18) Becker, D. P.; Barta, T. E.; Bedell, L. J.; Boehm, T. L.; Bond, B. R.; Carroll, J.; Carron, C. P.; DeCrescenzo, G. A.; Easton, A. M.; Freskos, J. N.; Funckes-Shippy, C. L.; Heron, M.; Hockerman, S.; Howard, C. P.; Kiefer, J. R.; Li, M. H.; Mathis, K. J.; McDonald, J. J.; Mehta, P. P.; Munie, G. E.; Sunyer, T.; Swearingen, C. A.; Villamil, C. I.; Welsch, D.; Williams, J. M.; Yu, Y.; Yao, J. Orally active MMP-1 sparing  $\alpha$ -tetrahydropyranyl and  $\alpha$ -piperidinyl sulfone matrix metalloproteinase (MMP) inhibitors with efficacy in cancer, arthritis, and cardiovascular disease. *J. Med. Chem.* **2010**, *53*, 6653–6680.
- (19) Gabelloni, P.; Da Pozzo, E.; Bendinelli, S.; Costa, B.; Nuti, E.; Casalini, F.; Orlandini, E.; Da Settimo, F.; Rossello, A.; Martini, C. Inhibition of metalloproteinases derived from tumours: new insights in the treatment of human glioblastoma. *Neuroscience* **2010**, *168*, 514–522.
- (20) Nuti, E.; Casalini, F.; Santamaria, S.; Gabelloni, P.; Bendinelli, S.; Da Pozzo, E.; Costa, B.; Marinelli, L.; La Pietra, V.; Novellino, E.; Bernardo, M.; Fridman, R.; Da Settimo, F.; Martini, C.; Rossello, A. Synthesis and biological evaluation in U87MG glioma cells of (ethynylthiophene)sulfonamido-based hydroxamates as matrix metalloproteinase inhibitors. *Eur. J. Med. Chem.* **2011**, *46*, 2617–2629.
- (21) Hagemann, C.; Anacker, J.; Haas, S.; Riesner, D.; Schömig, B.; Ernestus, R. I.; Vince, G. H. Comparative expression pattern of Matrix-Metalloproteinases in human glioblastoma cell-lines and primary cultures. *BMC Res. Notes* **2010**, *3*, 293.
- (22) Olson, M. W.; Bernardo, M. M.; Pietila, M.; Gervasi, D. C.; Toth, M.; Kotra, L. P.; Massova, I.; Mobashery, S.; Fridman, R. Characterization of the monomeric and dimeric forms of latent and active matrix metalloproteinase-9. Differential rates for activation by stromelysin 1. *J. Biol. Chem.* **2000**, *275*, 2661–2668.
- (23) Cha, H.; Kopetzki, E.; Huber, R.; Lanzendorfer, M.; Brandstetter, H. Structural basis of the adaptive molecular recognition by MMP9. *J. Mol. Biol.* **2002**, *320*, 1065–1079.